Study on the higher harmonic waves over a submerged bar

Bin Teng[1], Li-fen Chen[1], De-zhi Ning[1], Wei Bai[2]

1. Department of Hydraulic Engineering, Dalian University of Technology, Dalian, 116024,China
2. Department of Civil Engineering, National University of Singapore, 117576, Singapore
e-mail: bteng@dlut.edu.cn, chenlifen239@163.com, dzning@dlut.edu.cn, cvebw@nus.edu.sg

INTRODUCTION

The incoming waves propagating over a submerged structure may, in addition to being diffracted, generate higher harmonic waves due to wave shoaling effect. The generation of the super harmonic waves changes the swell spectrum because a significant part of the incoming wave energy may be transferred to higher frequencies. The higher harmonic waves may debase sailing conditions and do harm to coastal structures, so it is necessary to take account of their effects. The relating experimental and numerical studies can be seen for submerged plates and cylinders (Grue, 1992; Brossard and Chagdali, 2001; Liu et al. 2009), but the analysis of the higher-order harmonic waves scatting by submerged bar is relatively scare.

In this paper, the monochromatic wave over a submerged bar is investigated using a fully nonlinear numerical scheme based on a higher-order boundary element method (HOBEM). The phase-locked and free higher harmonic modes downstream the structure are decomposed by means of a two-point method, and their characteristics are further studied.

NUMERICAL MODEL

For wave overtopping a submerged bar (Fig. 1), a Cartesian coordinate system *Oxyz* is defined with the origin *O* in the plane of the undisturbed free surface. Fluid is assumed to be ideal, so that a velocity potential $\varphi(x, y, z, t)$ exists and satisfies the Laplace equation inside the fluid domain Ω. On the instantaneous free surface, both the fully nonlinear kinematic and dynamic boundary conditions are satisfied. On the solid boundaries (lateral walls and bottom), the rigid and impermeable condition is imposed. On the inflow boundary S_I the fluid motion is generated by prescribed second-order Stokes wave velocity. Towards the end of the computational domain, an artificial damping beach is applied on the free surface so that the wave energy is gradually dissipated in the direction of wave propagation.

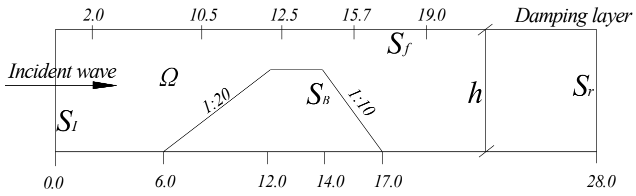

Fig.1 Sketch of wave propagating over a submerged bar

By using the second Green's theorem, the prescribed boundary value problem can be transformed the following boundary integral equation:

$$\alpha(p)\phi(p) - \int_{S_I+S_B} \phi(q)\frac{\partial G(p,q)}{\partial n}dS + \int_{S_f} G(p,q)\frac{\partial \phi(q)}{\partial n}dS = -\int_{S_I+S_B} G(p,q)\frac{\partial \phi(q)}{\partial n}dS + \int_{S_f} \phi(q)\frac{\partial G(p,q)}{\partial n}dS \quad (1)$$

where p and q are source and field points, and $\alpha(p)$ is the solid angle. For the Green function G, an image Green function is utilized so that the integration surface only includes the incident boundary and the free surface boundary and submerged bar S_B. The Green function can be obtained by the superposition of the image of the Rankine source about the sea bed and the infinite images about the two lateral walls and written as (Newman, 1992):

$$G(\vec{\xi},\vec{x}) = -\frac{1}{4\pi}[G_C(x-x_0, y-y_0, z-z_o) + G_C(x-x_0, y+y_0, z-z_o) + G_C(x-x_0, y-y_0, z+z_o+2h) + G_C(x-x_0, y+y_0, z+z_o+2h)] \quad (2)$$

where

$$G_c(X,Y,Z) = 1/\sqrt{X^2+Y^2+Z^2} + \sum_{n=-\infty}^{\infty}\left(1/\sqrt{X^2+(Y+2nB)^2+Z^2} - 1/2nB\right)$$

B is the tank width, and h is the water depth.

Then the boundary surface is discretized with a number of elements. The geometry of each element is represented by the shape functions, thus the entire curved boundary can be approximated by a number of higher-order elements. Within the boundary elements, physical variables are also interpolated by the same shape functions, i.e. the elements are isoparametric. In the integration process, the solid angle, the single layer and double layer integration are directly resolved (Teng, et al, 2006).

Since the discretized integral equation is always variant in time, all the boundary surfaces are regridded and updated at each time step using the mixed Eulerian-Lagrangian scheme and 4th-order Runga-Kutta approach. Once the Eq. (1) is solved, we can obtain the time history of surface evaluation at any position.

After waves pass the submerged bar, higher-order harmonic waves generated by nonlinear wave-wave interactions in the shallow water over the bar will leave the bar leeward as free waves. So the surface elevation at x in the lee side of the bar can be written as

$$\eta(t,x) = \sum_{n=1}^{\infty} a_n^{(F)} \cos(k_n x - n\omega t + \psi_n(x)) + \sum_{n=2}^{\infty} a_n^{(L)} \cos(n(kx - \omega t + \psi_1(x))) \tag{3}$$

where $a_n^{(F)}$ is the amplitudes of the free transmitted waves with frequencies of integer times of the incident wave frequency; $a_n^{(L)}$ are the amplitudes of the nth-order phase-locked waves, $\psi_1(x)$ are the initial phase angles of the fundamental waves and $\psi_n(x)$ $(n \geq 2)$ the nth harmonic free waves; k and k_n are the wave number of the fundamental waves and the nth harmonic free waves, and satisfy the following dispersion relations

$$\omega^2 = gk \tanh kh \tag{4}$$

and

$$(n\omega)^2 = gk_n \tanh k_n h, \quad n = 2,3,\text{L} \tag{5}$$

respectively. The fundamental wave amplitude, as well as the higher-order free and locked wave amplitudes, is obtained from the time histories of the surface elevation. The Fourier transform is introduced as follows

$$\eta_n(x) = \frac{2}{T}\int_0^T \eta(x,t) e^{-inwt} dt = A_n(x) + iB_n(x) \tag{6}$$

where $A_n(x)$ and $B_n(x)$ are the corresponding real and imaginary components, respectively.

Substituting Eq.(3) into Eq.(6) and making use of orthogonality of trigonometric function, we may obtain

$$a_1^{(F)} = \sqrt{A_1^2(x) + B_1^2(x)} \tag{7}$$

$$\psi_1(x) = ac\tan\frac{A_1(x)}{B_1(x)} - kx \tag{8}$$

$$a_n^{(L)} \cos(kx + \psi_1(x)) + a_n^{(F)} \cos(k_n x + \psi_n(x)) = A_n(x) \tag{9}$$

$$a_n^{(L)} \sin(kx + \psi_1(x)) + a_n^{(F)} \sin(k_n x + \psi_n(x)) = B_n(x) \tag{10}$$

Then we can obtain the amplitudes of the nth order locked waves and free waves after applying two fixed points' (Δx apart) surface elevations into Eqs.(9) and (10).

NUMERICAL RESULTS

As an example, the case for monochromic wave propagating a submerged bar as shown in Fig.1 was considered in this paper. The same problem were ever experimentally studied by Bej and Battjes (1993) and Luth etal. (1994). In the present numerical simulation, some parameters for wave period T=2.02s, wave amplitude A=0.01m and water depth h=0.4m are used. The corresponding computational domain is taken as $9\lambda \times 0.12\lambda$ ($\lambda=2\pi/k$ denotes wave length), meshed with 200×2 cells, in which the last 1.5λ is used as the damping layer. As the image Green function is used in the computational domain, meshes are only discretized on the surfaces of incident boundary, free surface and submerged bar, as shown Fig.2.

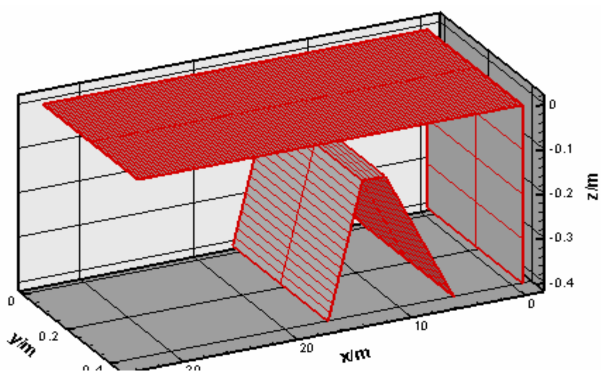

Fig.2 Meshes used in the computational domain

The comparisons of wave elevation time series at specific points (x=2.0m, 12.5m, and 19.0m) among the present results, experimental data and the solutions of the extended Boussinesq model of Nwogu (1993) are given in Fig.3. From the figures, it can be seen that there are good agreements for the three methods at points *x*=2.0m and 12.5m. But for the point *x*=19.0m, the Boussinesq model can't give accurate description because the wave nonlinearity is stronger behind the shoal. Therefore, the fully nonlinear model, such as the present scheme, is advised to analyze such problem.

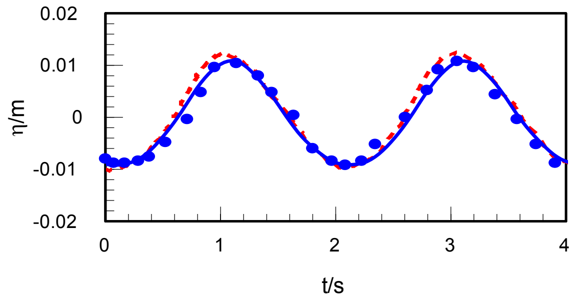

(*a*) *x*=2.0m

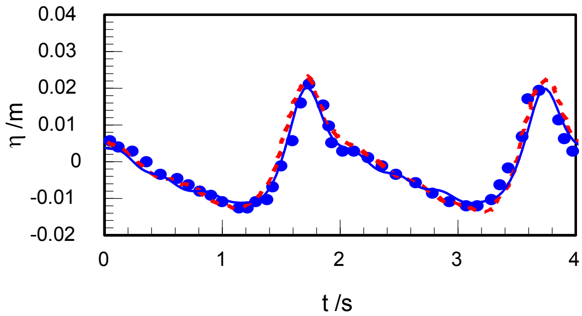

(*b*) *x*=12.5m

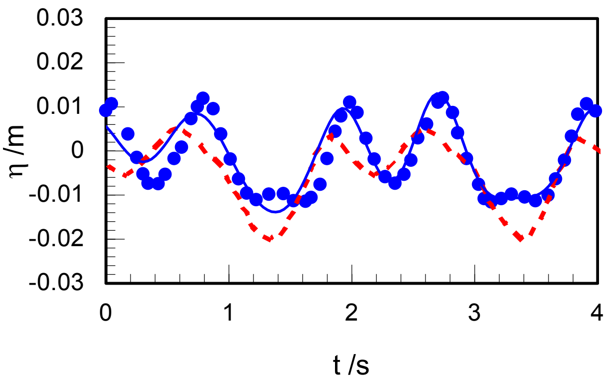

(*c*) *x*=19.0m

Experiment   Boussinesq   Present

Fig.3 Comparisons of free surface displacement among the experiment, Boussinesq model and present method.

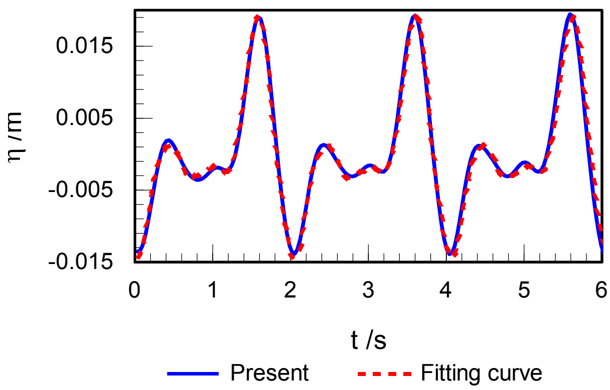

Fig.4 Comparison of free surface between the numerical solution and the fitting curve.

The results in Fig. 3 show that more higher-order harmonic waves are involved at the lee side of the submerged bar. So it is necessary to analyze these higher-order harmonics. Eq.(3) is used to separate various waves at point *x*=25.75m by truncating *n* to 7. The downstream neighbouring point is also used here for solving Eqs.(9) and (10). Fig.4 gives the comparison of free surface at point *x*=25.75m between the former one and the fitting curve. It proves the validity of the present method from good agreement.

Once the parameters $a_n^{(L)}$, $a_n^{(F)}$ and initial phase angles are solved, the various order wave records can be obtained as shown in Fig.5. From the figure, it can be seen that the periods of second and third-order waves are corresponding to 1/2 and 1/3 times wave period and phase-locked waves and free waves keep same periods but different phases. Locked waves are released to the corresponding free wave in a large degree after the wave propagating over the submerged bar.

Keeping the submerged bar unchanged, similar simulations have been carried out for different incident waves and water depths.

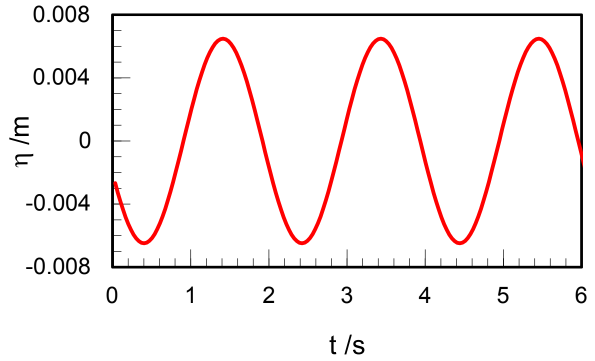

(a) Fundamental wave

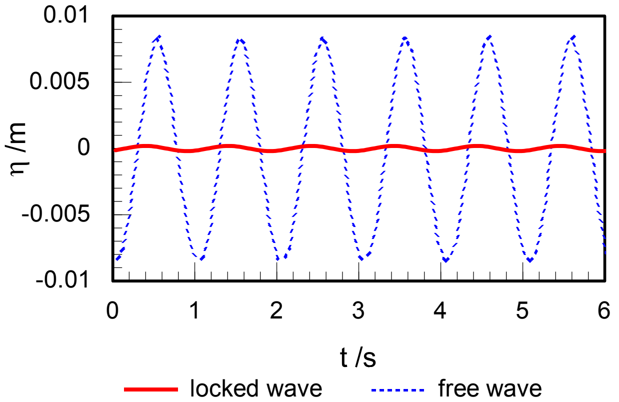

(b) 2nd-order waves

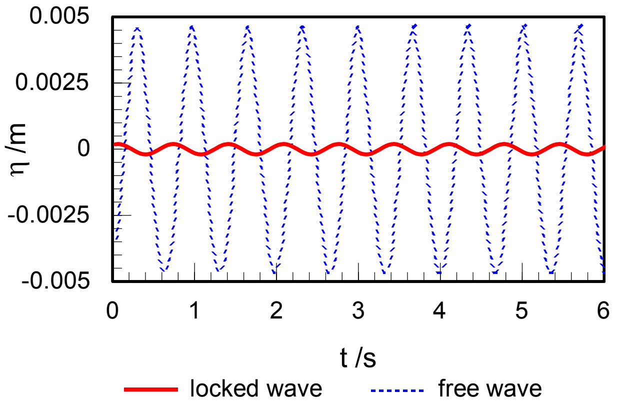

(c) 3rd-order waves

Fig.5 Time histories of various order waves

CONCLUSIONS

The phenomenon of wave propagation over a submerged bar is examined by a powerful numerical wave tank method. The transmitted waves are separated into the free waves and the locked waves with different harmonic frequencies. Numerical example shows that at the leeside of the bar the components of the free waves is much larger than the locked waves with the same frequency

ACKNOWLEDGEMENTS

The authors gratefully acknowledge the financial support from China NSFC (Grant Nos. 10772040, 50709005, 50921001) and the Major National Science and Technology Projects of China (Grant No. 2008ZX05026-02).

REFERENCES

Beji S., Battjes J.A (1993). "Experimental investigations of wave propagation over a bar". Coastal Engineering, 19, pp: 151-162.

Brossard J and Chagdali M (2009)."Experimental investigation of the harmonic generation by waves over a submerged plate". Coatal Engineering, 42, pp: 277-290.

Grue J (1992). "Nonlinear water waves at a submerged obstacle or bottom topography." Journal of Fluid Mechanics, vol. 244, pp. 455-476

Liu C R, Huang Z H, Tan S K(2009). "Nonlinear scattering of non-breaking waves by a submerged horizontal plate: Experiments and simulations" Ocean Engineering, 36, pp: 1332-1345.

Luth, H.R., Klopman, G., Kitou, N(1994). "Kinematics of waves breaking partially on an offshore bar; LDV measurements of waves with and without a net onshore current". Report H-1573, Delft Hydraulics.

Newman J N (1992). "Approximation of free-surface Green functions". In: P. A. Martin & G. R.Whickham (eds), Wave Asympotics. Cambridge University Press, pp. 107-142.

Nwogu, O (1993). "An alternative form of the Boussinesq equations for nearshore wave propagation". J.Waterway, Port, Coast, Ocean Eng. 119, 618–638.

Teng B, Gou Y and Ning DZ (2006). "A Higher Order BEM for Wave-Current Action on Structures—Direct Computation of Free-Term Coefficient and CPV Integrals," China Ocean Engineering. Vol.20, No.3, pp 395-410.